J Therm Anal Calorim (2012) 110:647–659
DOI 10.1007/s10973-011-1877-y

A review on the thermal stability of calcium apatites

Kaia Tõnsuaadu · Kārlis Agris Gross · Liene Plūduma · Mihkel Veiderma

Received: 17 June 2011 / Accepted: 17 August 2011 / Published online: 3 September 2011

Abstract High temperature processing is essential for the preparation of apatites for biomaterials, lighting, waste removal and other applications. This requires a good understanding of the thermal stability and transitions upon heating. The most widely used is hydroxyapatite (HAp), but increasing interest is being directed to fluorapatite (FAp) and chlorapatite (ClAp). The structural modifications for substitutions are discussed to understand the temperature processing range for the different apatites. This is based on a review of the literature from the past few decades, together with recent research results. Apatite thermal stability is mainly determined by the stoichiometry (Ca/P ratio and structural substitutions) and the gas composition during heating. Thermal stability is lowered the most by a substitution of calcium and phosphate, leading to loss in phase stability at temperatures less than 900 °C. The anions in the hexagonal axis, OH in HAp, F in FAp and Cl in ClAp are the last to leave upon heating, and prevention of the loss of these groups ensures high temperature stability. The information discussed here will assist in understanding the changes of apatites during heating in calcination, sintering, hydrothermal processing, plasma spraying, flame pyrolysis, and other high-temperature processes.

Keywords Calcium apatite · Thermal stability · Structural substitutions · Sintering · Thermal analysis

K. Tõnsuaadu (✉) · M. Veiderma
Laboratory of Inorganic Materials, Tallinn University of Technology, Ehitajate tee 5, 19086 Tallinn, Estonia
e-mail: kaiat@staff.ttu.ee

K. A. Gross · L. Plūduma
Riga Biomaterials, Innovation and Development Centre, Riga Technical University, Pulku 3-3, Riga 1007, Latvia
e-mail: kgross@rtu.lv; karlis.gross@eng.monash.edu.au

L. Plūduma
e-mail: liene.pluduma@rtu.lv

K. A. Gross
Department of Materials Engineering, Monash University, Melbourne, VIC 3800, Australia

Introduction

The multifunctionality of calcium apatite is attributed to a large capability for elemental substitution, the active surface and a range in crystal perfection (low to high crystallinity). Harnessing these attributes provides a propensity to many applications, but relies on the improved processing–microstructure–property relationship, considered being important for the design and tailorability of material properties.

The best starting point for altering the characteristics of apatites is with high crystallinity apatites. These are most frequently produced by high-temperature processing, a common approach for calcining and product manufacture. The crystalline structure provides the best capability to understand the chemical and structural make-up of the apatite. The study and further use of apatites thus requires a degree of thermal stability, and is the basis of this review.

Apatite structure

Apatites are a diverse group of minerals found in rocks (igneous rocks and some metamorphic and sedimentary rocks), as well as the main inorganic constituent of natural hard tissues. Synthetic hydroxyapatite (HAp) is used as a biomaterial for orthopaedic and dental applications in the pure or chemically modified form. The basic formula of

apatite is $Ca_{10}(PO_4)_6X_2$ where X is F, Cl or OH. Natural apatite usually consists of a solid solution of these anions, with hydroxyl groups being always present. The composition of apatite, however, is even more variable because a large number of different species can be substituted into the structure [1, 2]. The most common apatite structure has a hexagonal symmetry $P6_3/m$. The lattice parameters of apatite crystals depend on the chemical substitutions [3, 4].

Substitutions modify the structure and often show marked effects on characteristics, such as crystallinity and other properties (solubility, mechanical, thermal stability, optical, and bioactivities) [5–7]. The effects of different ionic substitutions on the bio-HAp have been discussed in numerous articles and in an overview by LeGeros [8].

Apatites can have extensive substitution of all groups [1, 2], but the apatite class will always include calcium and phosphate groups. The degree of substitution leads to an array of different apatites that need appropriate abbreviations. To indicate the substitution, the element or chemical group will be placed in front of the particular apatite name abbreviation. For example, a magnesium- and carbonate-substituted fluorapatite will be written as $MgCO_3FAp$. The abbreviations used in this study are shown in Table 1.

There are several crystallographic sites where atomic exchanges can occur, allowing elements with different ionic charges to be taken up into the lattice [1, 3, 9]. The scope of these substitutions is interpreted the best way in an onion diagram, representing the base apatite (fluorapatite, chlorapatite and hydroxyapatite) in the inner circle, Fig. 1. Iodoapatite and bromapatite have not been included since the large I^- and Br^- ions are more difficult to incorporate. Solid solutions can exist between these apatite classes. The next inner layer represents anionic substitutions, replacing PO_4, given in the order of decreasing substitution capability. The remaining onion layers represent the monovalent, divalent and trivalent cation substitutions. Sodium substitutes favour in minor quantities for the other ions substitution, only occurring as trace elements. Divalent cations may completely substitute for calcium with a tendency for higher substitution levels in ClAp and HAp than FAp [1]. After divalent substitutions, the trivalent ions can be substituted in significant quantities. This study will not address the trivalent cation substitutions.

Table 1 Abbreviations for the different apatites and decomposition products

Class of apatite	Chemical modifications
FAp	FHAp, CO_3FAp, ZnFAp, MgFAp, $NaMgCO_3$FAp
ClAp	ClAp, ClHAp
HAp	OHAp, OAp, Ca def HAp,
CO_3Ap	A-CO_3Ap, B-CO_3Ap, AB-CO_3Ap
*xy*HAp	A HAp with *x* and *y* as substitutions
bioAp	A wide range of substitutions
$Ca_3(PO_4)_2$	TCP—tricalcium phosphate can form a α- or β-phase
$Ca_4(PO_4)_2O$	TTCP—tetracalcium phosphate

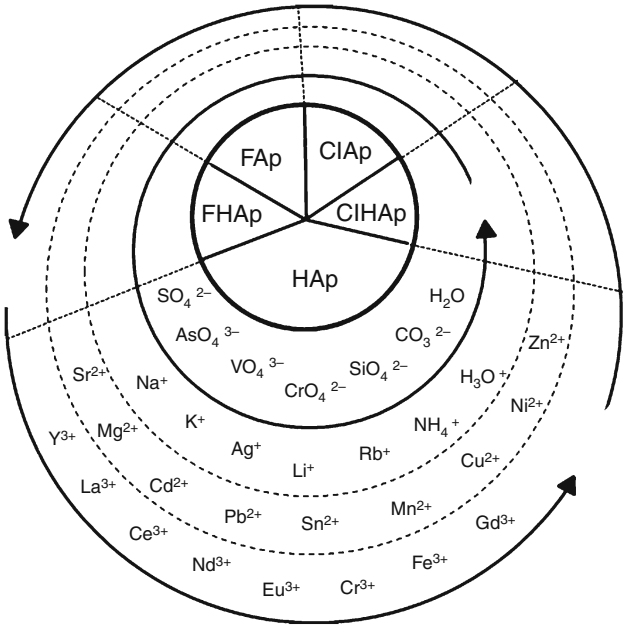

Fig. 1 An onion diagram representing the core apatites in the centre and substitution elements in different layers. The inner layer contains anionic substitutions, but the outer layers provide the monovalent, divalent and trivalent cationic substitutions. The ions are shown in an approximate decreasing ability of substitution

Thermal processing

Heating is applied to process apatites for a wide range of applications. Thermal processing is used for production of multiple calcium phosphates or for improving the crystallinity. Fluorides containing natural apatite minerals are mainly used in the fertilizer and phosphorus industries [10, 11]. Temperatures above 1200 °C are used in hydrothermal processes to obtain fluoride-free phosphates [12, 13]. These are complex processes involving the participation of impurity minerals in apatite concentrates [14, 15]. Natural bio-apatites (wastes from food production), heated for purification, have been proposed for the removal of heavy metals from contaminated soils [16].

The properties of synthetic apatites produced by precipitation depend not only on the reactants, solution pH, rinsing, but also on the synthesis temperature that will affect the crystallinity and crystal size [17]. Sol–gel synthesis when organic precursors are used requires thermal treatment up to about 700 °C for the removal organic components [18]. Coatings made by plasma spraying rely on feedstock thermal stability for producing the desired

final phase composition [5, 18, 19]. These thermal treatments all influence the properties of apatite.

Thermal stability of synthetic hydroxyapatite is of great importance to control sintering or thermal processing conditions for the design and preparation of hydroxyapatite ceramics. Calcination is an important process for conditioning synthetic HAp for further processing. Low crystallinity powders can evolve gases leading to undesirable internal pores in sintered ceramics, but higher crystallinity powders require a higher temperature before shrinkage begins [20]. Decomposition at higher temperatures is preferably avoided, since the prior release of gases drastically reduces the strength [21].

The objective of this article is to collate information on apatite thermal stability with respect to the chemical composition, particularly the hexagonal axis ions involving OH^-, F^- and Cl^-, and structure. The focus of this study will address the structural rearrangements and changes in chemistry where either the calcium or phosphate groups are replaced upon heating. In the case where no reference is made to the atmosphere, it is assumed that heating is conducted in air.

Test methods for thermal stability

Phase changes and decomposition of apatites are studied by means of thermal analysis. This includes thermogravimetric analysis (TG), differential thermal analysis (DTA), calorimetry, high-temperature X-ray diffraction, microscopy, and dilatometry. TG and DTA may be combined with evolved gases analysis (EGA) by mass spectrometry (MS), Fourier transform infra-red spectroscopy (FTIR) or gas chromatography. The simultaneous analysis of the gaseous products provides additional information about thermal events, such as evolved species, the amount and evolution rate versus time. It supplies a comprehensive understanding of thermal changes in a reliable and meaningful way allowing a thermal event to be matched with the evolved gas species.

Thermal response depends on the heating rate, amount of sample, particle size, phase purity, etc. [22] and must be taken into consideration when interpreting the results. The composition and pressure of the environment are important for solid–gas reactions, especially for apatites.

Since the crystalline structure is just as important as its chemical composition, both characteristics should be provided where possible. Calcium phosphate phases, before and after calcination, can be characterized and distinguished from each other with X-ray diffraction (XRD), FTIR, Raman, and NMR spectroscopy. Crystal size can be determined by XRD [23], or electron microscopy, but shape requires observation with scanning electron microscopy (SEM) or atomic force microscopy.

Thermal analysis in analytical methods

At present, there are only two methods that have been suggested as possible analytical methods. These provide the hydroxide and hydrogen phosphate contents. Both are related to the change in apatite mass upon heating.

It has been shown that a mechanical blend of HAp and CaF_2 heated to 800 °C results in replacement of OH^- with F^- ions and a resultant evolution of water, proved by XRD and IR spectroscopy analyses. The weight loss may be attributed to the OH^- content [24], as shown in Fig. 2. The presence of carbonate should be considered, and the weight loss from CO_2 subtracted. It is better applied to high-temperature processed apatites that have released all absorbed species and any other gases that will otherwise interfere with the weight loss within the preferred temperature interval of 500–800 °C.

For calcium phosphates that contain HPO_4^{2-}, a weight loss between 400 and 700 °C occurs after forming pyrophosphate with the evolution of water [31]. As pointed out by Elliot, above 700 °C, the calcium pyrophosphate reacts with HAp to produce TCP and water [3, 25]. The suggested temperature to measure the hydrogen phosphate concentration is 600 °C. More detailed information on the purity of apatites coupled with thermal analysis will provide means of more closely determining other changes that occur upon heating apatites.

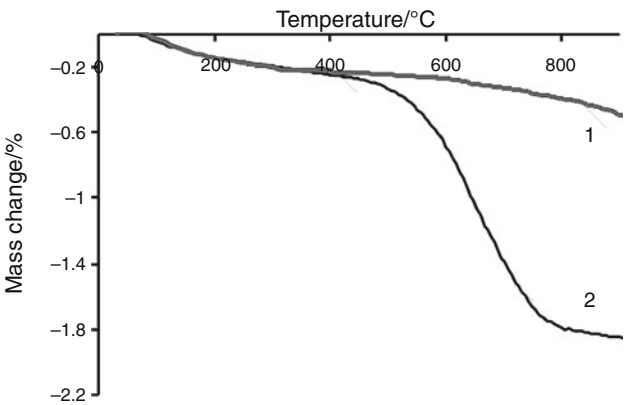

Fig. 2 Thermogravimetric analysis of HAp–CaF_2 mixture, with an excess of CaF_2 to form FAp. The weight loss between 420 and 800 °C provides an OH content of 1.7% for a completely hydroxylated HAp with a Ca/P ratio of 1.67. 1 HAp; 2 HAP-CaF_2 mixture. The run was performed at Tallinn TU in a Setsys TG/DTA (Setaram, France). A heating rate of 10 deg min^{-1}, an Ar flow of 60 mL min^{-1} and a 100 μL Pt crucible were used

Changes in apatites with heating

The thermal properties will be discussed, starting with the main stoichiometric apatites, followed by anionic substitutions, and then cationic substitutions as shown in Figure 1. Pure apatites with only one type of anion in the hexagonal axis are very rare. Hereby, the data on pure apatites are more theoretical, and intended as a reference. The stability of apatite is determined by the anion position in the hexagonal axis and decreases in the following order F > Cl > OH [4].

Unfortunately, the sample's composition is often reported in insufficient detail and XRD is unable to reveal all the structural substitutions, particularly for very fine crystal sizes that produce peak broadening, and so this will lead to variability in values stated in the literature.

Stoichiometric apatites

Fluorapatite

Fluorapatite (FAp), the most stable of all the apatites with fluoride being the most negative and small enough to be positioned within the calcium triangle, melts at 1644 °C, and decomposes in a dry atmosphere according to the following reaction [26]:

$$3Ca_{10}(PO_4)_6F_2 \rightarrow 2POF_3 + 2Ca_3(PO_4)_2 + 6Ca_4(PO_4)_2O \quad (1)$$

The FAp-CaF_2 phase diagram prepared by Prener [27] shows that a liquid phase is formed at 1203 °C. A recent study on synthetic FAp whiskers, obtained by high-temperature synthesis (1175 °C) with a Ca/P = 1.643, confirms FAp stability up to 1200 °C [28].

Chlorapatite

Chlorapatite (ClAp) is reported being more stable than HAp [4]. It undergoes a phase change from hexagonal to monoclinic upon heating at 200–300 °C [3, 29] and is stable to 1200 °C at which point cracks, pores and large grains are observed [30]. The poor sinterablity of ClAp produces a lower three-point bend strength compared to HAp. Heating in a vacuum between 900 and 1200 °C for 16 h will lead to a partial loss of the chloride ions [31]. The loss of the column anions is common for all apatites upon heating.

Plasma spraying of HAp has been compared to ClAp showing that less amorphous calcium phosphate and oxyapatite is formed from ClAp powder [29]. The above discussion suggests that the thermal stability decreases from FAp to ClAp and further to HAp. A comparison of all three materials is still not available, and requires further investigation, with a detailed knowledge of the anion concentration, any replacement column anions and the trace element concentrations.

Hydroxyapatite

Thermal events followed during thermal treatment of HAps depend on the obtaining conditions. Precipitated HAp exhibits two to four stages of mass loss in the low temperature region, up to 500 °C [25, 32–34]. Precipitated HAp has two types of water—adsorbed water and lattice water [8, 35]. Adsorbed water is reversibly removed from 25 to 200 °C without any effect on lattice parameters. There is an outer physisorbed layer and an internal chemisorbed monolayer. The physisorbed water is released at lower temperatures, whereas more energy is required to release the chemisorbed water. Active researches are addressing the effect of different crystal surfaces and surface chemistry of apatite crystals [36, 37]. Water in pores, cracks and inter-crystallite locations is stabilized by capillary effects and requires higher temperatures for release. Lattice water is irreversibly lost between 200 and 400 °C, which cause a contraction in the *a*-lattice dimension during heating [32]. Surface phosphorus is reactive and will readily form a P-OH that is dehydroxylated above 400 °C to form P-O-P surface groups [25].

Dehydroxylation of HAp begins at temperatures at about 900 °C in air and 850 °C in a water-free atmosphere [32, 34, 38, 39], Reaction 2.

$$Ca_{10}(PO_4)_6(OH)_2 \rightarrow Ca_{10}(PO_4)_6(OH)_{2-2x}O_x\square_x + xH_2O \quad (2)$$

where $\square_x$ is a hydrogen vacancy.

The decomposition of HAp is a process of continuous reactions, in which the conversion degree of dehydroxylation can strongly influence the critical temperature of subsequent decomposition [25, 34, 40]. When OH groups are removed from the HAp structure, two OHs combine to form one molecule of water, leaving a peroxy ion (O^{2-}) in the lattice:

$$2OH^- \rightarrow H_2O + O^{2-}$$

This is followed by a small weight loss as water leaves HAp and enters the gas phase. Dehydroxylation introduces vacancies to create oxyhydroxyapatite (OHAp) with a similar crystal structure to HAp. Bredig et al. [41] were the first to demonstrate the existence of OHAp in 1933 by heating at 1360 °C under vacuum for 7.5 h and produced a 55% dehydroxylated HAp. A 75% dehydroxylated HAp has been formed under vacuum and results extrapolated to 100% dehydroxylation to establish the lattice parameters of

oxyapatite (OAp; $Ca_{10}(PO_4)_6O$) [42]. Trombe showed that an A-type carbonated HAp can also be heated to remove carbonate ions from the channels as an alternative approach for oxyapatite preparation [42]. Oxyapatite has also been formed in a thermal spray coating, but the surface of the coating readily absorbs moisture to form a hydroxyapatite [19]. The preparation of an oxyapatite via a low-temperature amorphous phase could release water more easily since nanocrystals may be more effective in releasing the structural water and carbonate from the columns. A significant weight loss at above 1300 °C leads to a large removal of hydroxyl groups [43].

As HAp is slowly dehydroxylated, there is a decrease in lattice parameter, but this is more difficult to follow with XRD than changes in FTIR spectra that show a clear decrease in the OH band at 3570 cm^{-1} [44].

The range of temperature for OAp stability is very narrow around 800–1050 °C [33, 43]. Two outcomes of OAp decomposition above 1050 °C are stoichiometrically possible: a mixture of tetracalciumphosphate (TTCP) and tricalciumphosphate (TCP, β-TCP at temperatures below ~1200 °C and α-TCP at higher temperatures), or it may decompose to a mixture of TCP and CaO by the following reactions, and this does not involve any change in weight:

$$Ca_{10}(PO_4)_6O \rightarrow 2Ca_3(PO_4)_2 + Ca_4P_2O_9 \text{ and} \quad (3)$$

$$Ca_{10}(PO_4)_6O \rightarrow 3Ca_3(PO_4)_2 + CaO \quad (4)$$

The dehydroxylation of commercial Fluca HAp powder upon heating to 1250 °C in dry air flow has produced four successive conversion stages corresponding to different kinetic mechanisms, which were calculated by means of the Ozawa–Flynn–Wall method. According to the calculated activation energy–conversion degree plot, the kinetics of HAp dehydroxylation include four reaction-rate-controlling processes with different activation energies [34]:

(1) OH^- diffusion through HAp;
(2) OH^- debonding from HAp lattice;
(3) lattice constitution of OAp, and
(4) loss of surface water by $2OH^- \rightarrow H_2O\uparrow + O^{2-}$.

Effect of water vapour

FAp releases fluoride when heated in the presence of H_2O, even at small concentrations in air, above 1000 °C to form HFAp [13, 45]. The extent of defluoridation depends on the temperature, time and the water vapour pressure.

ClAp is less stable than FAp and will easily convert to HAp when heated in steam above 800 °C [24, 45]. Recent study has shown the inclusion of water vapour in a furnace can reduce the stability of ClAp and produce a transformation at 50 °C lower than in dry air. The transformation can be followed by the appearance of the (002) HAp peak at 26.1° [31].

A very important property of highly dehydroxylated HAp under a vacuum of 1.3 mPa at 1000 °C is that it could be rehydroxylated in a water vapour atmosphere [42] as low as 400 °C. It is particularly important to eliminate all traces of water when OAp is to be prepared.

The reconstitution temperature of HAp has been reported to be dependent on cooling rate and atmosphere [33, 46, 47]. Plasma-spraying has been shown to produce a large amount of TTCP and α-TCP and a small amount of CaO and $Ca_2P_2O_7$ [48].

Thermal spraying can readily produce dehydroxylation, but also amorphous phases from rapid cooling [47]. This amorphous phase content increases with less pure HAp [49]. Reheating ground HAp coatings in air containing water vapour results in recrystallization of the glass phase and formation of HAp at 600 °C [50]. Heating the coating in the presence of water vapour can crystallize hydroxyapatite at 500 °C. The lower temperature could arise from the residual stresses or the use of a high vapour pressure. Heating in the absence of moisture will lead to oxyapatite at 700 °C [47]. Post-heat treatment revealed that hydroxyapatite can be restored from hydration of TTCP and α-TCP at high temperatures and water content [48]. Hydrothermal treatment in an autoclave at temperatures as low as 200 °C can provide crystallization and also heal the cracks within the thermal spray coating structure [51].

When HAp (Merck) is heated to 1500 °C and then cooled, a high-temperature XRD study shows that a part of TTCP and α-TCP initially converted into OAp around 1350 °C and maintained during cooling until 1300 °C [32]. Upon cooling to 1290 °C, a part of TTCP and α-TCP converts to OHAp by rehydration with a significant weight increase. At 1100 °C, the rest of TTCP and α-TCP completely reconstitutes the HAp phase. OHAp then gradually rehydrates and reconstitutes HAp. This emphasizes the importance of the heat treatment regime on the change in microstructure that can lead to differences in the resulting material properties.

Instability of OHAp in the presence of water molecules explains the higher stability of HAp at calcination [52–54]. It was shown that in a moist atmosphere (in which water is explicitly added by bubbling gas through water at room temperature, partial pressure of water ~17.5 mm Hg) it is possible to sinter HAp up to a temperature of 1300 °C without dehydroxylation or decomposition [38]. However, in theory, it should be possible to sinter HAp with a Ca/P ratio of precisely 1.67 to temperatures up to 1475 °C before decomposition begins, provided that the partial pressure of water in the sintering atmosphere is 500 mm Hg [55]. In

the case of 'pressure-less' sintering, gas needs to be bubbled through water very close to boiling [40].

Hexagonal anion substitutions

Theoretically, the crystal structure of F-OH apatite should be more regular [3] and have a higher thermal stability. XRD data of FHAp ceramics obtained from precipitated nanosized FHAp powders sintered at 1300 °C and TG data of the FHAp powders in the temperature range from 25 to 1300 °C, revealed a greater thermal stability of the HAp matrix and a greater resistance to decomposition when fluoride replaces more than 60% hydroxyl ions [39].

Carbonate substitution in hexagonal axis will be discussed in a section of carbonate substitution.

Phosphate substitutions

Ca/P ratio impact

Small deviations in the Ca/P ratio of the starting material result in the formation of secondary phases at heating. The substitutions of carbonate and hydrogen phosphate in the apatite structure have been found to lower the Ca/P to 1.62 [56, 57]. A lower Ca/P ratio lowers the crystallinity and accelerates the decomposition [58–60].

Acid phosphate (HPO_4) may be lost at 250–400 °C and form diphosphate ($Ca_2P_2O_7$), although Ca-def HAp exhibits this behaviour at 400–700 °C [57, 61]. At temperatures above 700 °C, Ca-diphosphate reacts with HAp to give β-$Ca_3(PO_4)_2$ [62, 63].

The newly formed β-TCP in turn accelerates the decomposition of HAp. A study of HAp produced by a solid-state reaction and mixed with β-TCP revealed that the presence of β-TCP strongly affects the post-sinter HAp/β-TCP ratio by promoting the thermal decomposition of HAp to β-TCP, even at sintering temperatures as low as 850 °C. Hydroxyapatite content also influences the reverse transformation of α-TCP to β-TCP [63].

Apatite with a Ca/P ratio greater than 1.667 gives HAp and CaO on heating above 900 °C [3]. On cooling, the CaO may react in the atmosphere to form $Ca(OH)_2$ and/or $CaCO_3$.

Carbonate substitution

Carbonate ions in the apatite structure either substitute OH^- ions to form an "A-type" carbonated hydroxyapatite or PO_4^{3-} to form a "B-type" substitution [3]. The "B-type" substitution referred to as B-CO_3Ap is more common, but more complex than the "A-type" carbonated hydroxyapatite, herein referred to as A-CO_3Ap.

B-CO_3Ap has a complex defect structure involving possibly two types of water within vacancies of the apatitic mineral crystal, and this stabilizes the apatite structure [35, 56, 64]. The carbonate substitution could also be stabilized by other substitutions such as CO_3OH, H_3O^+, HPO_4^{2-}, Na^+ or NH_4^+ depending on the synthesis conditions [3, 65]. Pure A-type carbonated apatites may be prepared by heat treatment of HAp for several hours in a CO_2 atmosphere between 800 and 1000 °C [66]. Synthesized precipitates are usually combined A- and B-type carbonated apatites (AB-CO_3-Aps). This type of structure is obviously less stable, and its decomposition is very complicated [67].

Thermal changes in CO_3Ap are illustrated in Figure 3 that shows an evolution of gases (Fig. 3a), the corresponding weight loss from a similarly shaped dm/dT curve (Fig. 3b), and the change in lattice parameters (Fig. 3c):

(1) The evolution of adsorbed water starts at 90° C and the water bound in the apatite structure evolves up to 500 °C [54]. A decrease in lattice constants *a* and *c* (Fig. 3c) suggests rearrangements in the structure [35]. An accompanying release of ammonia in the EGA curve (Fig. 3a) is observed for the apatite synthesized from ammonium-containing reactants, confirming that all weight loss up to 400 °C cannot be solely attributed to the release of water [68].
(2) A loss of carbonate in air, an endothermic reaction, starts at 400–500 °C and is completed at 800–1200 °C [69] or between 630 and 1250 °C [70]. Carbonate evolution at 300–600 °C has been attributed to a reaction between hydrogen phosphates and carbonates [54] or carbonate structural relocation [3, 35]. Another study that measured the lattice parameters and monitored the evolved gas with mass spectrometry showed decarbonisation of A sites at 450–600 °C and B sites at 75–950 °C [65]. The release of carbonate from B sites (Fig. 3a) arising from synthesized hydroxyapatite also shows the increase in lattice parameter *a* (Fig. 3c).

The decarbonation of AB-CO_3Aps in air or an inert atmosphere starts from about 600 °C and proceeds in two steps at about 700 and 950 °C [71]. This behaviour is explained by different substitution modes for carbonates in the apatite. The temperature decreases for evolving carbonate with an increase in the carbonate content [72, 73].

(3) Decomposition of the apatite: The mass loss for CO_2 departure is slightly higher than the carbonate content of the initial powders. This is explained by the dehydroxylation at the A sites to evolve water and create OHAp [55, 74].

At about 1250 °C, the mass loss is attributed to the release of water from a reaction between the oxyhydroxyapatite and

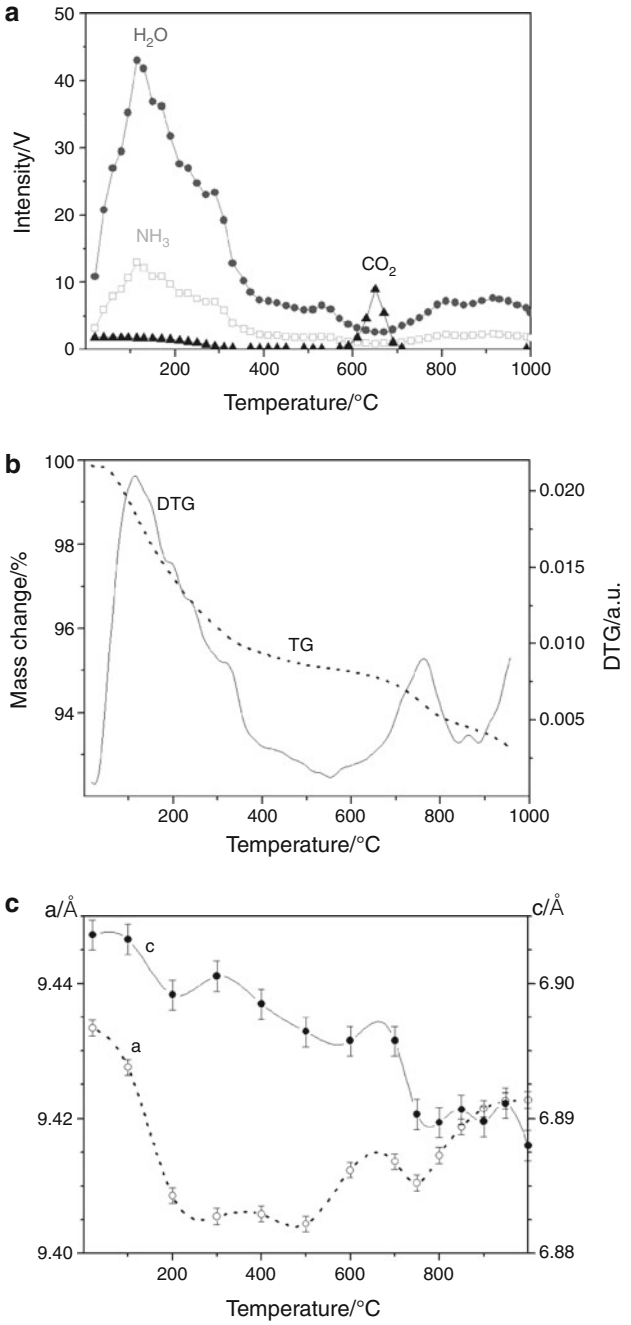

Fig. 3 Thermal analysis of a carbonated HAp showing **a** weight loss and differential weight loss, **b** evolved gases from a mass spectrometer, and **c** lattice parameters at different temperatures. The authors acknowledge access to the data supplied by Zyman et al. [73]

CaO to form tricalcium phosphate (observed in XRD patterns) according to the following reaction:

$$Ca_{10}(PO_4)_6(OH)_{2.2x}O_x + 2CaO \rightarrow 3Ca_4O(PO_4)_2 + (1-x)H_2O \quad (5)$$

At 1300 °C, the last TG peak is associated with the decomposition of the remaining OHAp into TCP phosphate and TTCP [57, 71]:

$$Ca_{10}(PO_4)_6(OH)_{2.2x}O_x \rightarrow 2Ca_3(PO_4)_2 + Ca_4O(PO_4)_2 + (1-x)H_2O \quad (6)$$

The sintering atmosphere appreciably influences the phase transformation and decomposition of carbonated apatite [75]. Use of a carbon dioxide atmosphere can protect CO_3HAp against thermal decomposition [67, 76]. A CO_2 gas partial pressure of 50 kPa stabilizes carbonated apatites up to sintering temperatures, but CO_2 gas induces carbonation of hydroxide sites (A-site) that is undesirable for sintering.

A low partial pressure of water vapour in the atmosphere controls A-site carbonation and indirectly favours sintering. Dense ceramics made of single-phased apatite $Ca_{10-x}(PO_4)_{6-x}(CO_3)_x(OH)_{2-x-2y}(CO_3)_y$, with $0 \leq x \leq 1.1$ and $0 \leq y \leq 0.2$ could be produced. The value of x (B-type carbonates) is controlled by the synthesis process and the value of y (A-type carbonates) by the sintering atmosphere [67].

Natural carbonated fluorapatite (CO_3FAp) begins to release CO_2 and F at about 520 °C for heavily carbonated samples, but requires temperatures closer to 800 °C for low carbonate content apatites [77]. This leads to the formation of FAp and CaO [78]. There is a systematic increase in the a-axis and crystallite size with a loss of carbonate [78, 79].

Loss of CO_2 and N_2 on heating CO_3FAp precipitated in the presence of ammonium salts has been investigated by gas chromatography [80, 81]. Carbon dioxide is evolved between 450 and 950 °C in three stages. The first stage at 480 °C is attributed to the decomposition of carbamate ($NH_2CO_2^-$), the second at ~700 °C to CO_3^{2-} and the third at ~800 °C to CO_3F or to CO_3OH substitutes.

Precipitated FHAp (pH 10) with a low carbonate content exhibits a higher thermal stability compared with HAp synthesized at the same conditions. Hydroxyapatite decomposes to α-TCP above 960 °C, whereas FHAp requires temperatures above 1300 °C for the loss in structure [82]. This is explained by the more ordered apatite structure of FHAp [39].

Sulphate substitution

Thermal analysis together with FTIR and Raman spectroscopies shows that recrystallization of precipitated sulphate apatites occurs almost at the same temperature interval as that of CO_3Aps, at 650–830 °C. In sulphate

apatites, the reaction is clearly exothermic without a marked mass loss, leading to $CaSO_4$ and pure apatite [83].

The presence of fluoride ions in A sites decreases the decarbonation temperature of B-CO_3Aps down to 500 °C [77, 84] and a transition of the sulphate ion [72].

Cationic substitutions

Sodium substitution

The thermal behaviour of Na-containing carbonated apatites [68, 75, 85–88] has shown very similar behaviour to $CaCO_3$Ap. Thermal stability of carbonate substitutions is a little higher when Na substituted apatite is calcined [87, 88]. Heating precipitated sodium containing CO_3Ap to 1000 °C causes decomposition to HAp, Na_2O and CaO**.** The composition will vary depending on the atmosphere (CO_2/H_2O or N_2/H_2O) [3].

Magnesium substitution

(a) in fluorapatite

Precipitated FAp with various Mg content (Ca + Mg/P = 1.6) dehydrates up to 480 °C, but decomposes to $Mg_2F(PO_4)$ and FAp above 650 °C [89]. Carbonated fluorapatite with Mg and Na substitution obtained by precipitation in presence of NH_4^+ was studied by means of TG-FTIR and XRD analyses [68]. The crystal structure of the precipitated Mg apatites is relatively labile; however, after release of volatiles at 1000 °C, a more stable and crystalline apatite forms. Water is evolved mainly before 500 °C in three or four steps when heated in He, followed by thermal effects producing a rearrangement of the structure. CO_2 is evolved over a wide temperature range, from 100 up to 800–1000 °C. Ammonia is evolved at 100–400 °C with a sharp peak at about 280 °C for Na containing samples. $CaMgCO_3$Ap exhibits some greater thermally stability in the presence of Na.

(b) in hydroxyapatite

A small amount of Mg (Mg/(Mg + Ca = ~6 mol%) may substitute for calcium in HAp synthesized by the precipitation method at 90 °C [90]. An increase in Mg content decreases the precipitated crystallite size, led to more irregular forms and agglomeration occurs. Magnesium is thought to destabilize the apatite structure. This can be explained by the severe strain from much smaller ions that introduces more defects and favours HAp decomposition upon heating.

CO_3Ap precipitated in the presence of Mg^{2+} evolves CO_2 at 350–905 °C. An exothermic response up to 400 °C provides energy for restructuring after the loss of water in Mg substituted HAp [72, 91]. High Mg contents in synthetic HAps (0.6 to 2.4 wt%) reduces the decomposition temperature from 840 to 660 °C to form a magnesium-substituted β-TCP or $(Ca,Mg)_3(PO_4)_2$ [92]. The incorporation of Mg promotes the formation of β-TCP phase and stabilizes the β-polymorph up to 1300–1400 °C [91, 92]. Inclusion of sodium in Ca–Mg CO_3Ap appears to slightly increase the thermal stability [68].

Other cationic substitution

Other cationic substitutions also decrease the HAp stability. The degree of CaMnHAp decomposition depends on the amount of Mn and the calcination temperature. Hydroxyapatite with 0.1–1.0 wt% Mn does not decompose until 800 °C. MnHAp containing 5.0 wt% Mn decomposes at 800 °C to α-TCP and β-TCP with the formation of Mn_3O_4 as a secondary phase. After heat treatment at 1250 °C, complete decomposition of HAp-Mn 5.0 wt% produces α-TCP [93, 94]. Similar behaviour occurs when HAp is modified with Zn [95–98], Ni [99], and Cd [100, 101].

CaZnFAp with Ca + Zn/P = 1.9 precipitated from ammonia salts contains a max of 25 atomic percent of Zn, but a mixture of phases at higher Zn contents. The highly non-stoichiometric apatitic phosphate is stable up to 500 °C, but a new phase $CaZn_2(PO_4)_2$ is formed at higher temperatures. Thermal stability of these samples decreases with increasing Zn concentration possibly because of the repulsion of small zinc ions from some of the cationic positions in the FAp structure [102].

Unfortunately comparison of the impact of different metallic substitution, based on published data, is complicated due to the different levels of substitution and the use of different analytical techniques.

Bioapatites

The mineral component of bone is generally agreed to be based upon the apatite mineral structure. Bone mineral contains a substantial amount of carbonate ion (5–8%), mainly located in phosphate lattice positions. It is calcium deficient, often containing Na, K, Mg, and Zn substitutions with possible vacancies. Very few hydroxyl groups occupy the apatite in bone [103, 104]. However, enamel has less carbonate, and a higher concentration of hydroxyl ions. Thermal behaviour of biological apatite (enamel, dentine and bone mineral) has been extensively studied [8, 105–109] also reporting the effect of heating atmospheres [75, 110].

Weight loss of bioAp from calcination can be observed at three stages:

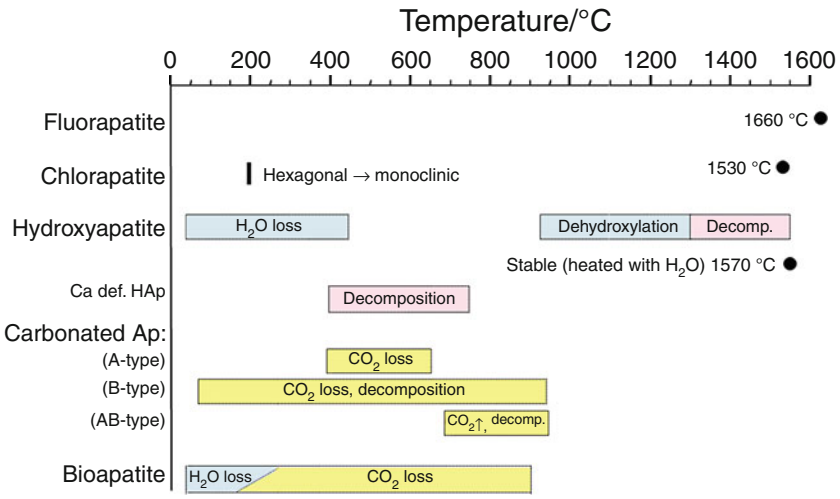

Fig. 4 Thermal events for apatites (FAp, ClAp, HAp, CO_3Ap, BioAp) showing a phase change (ClAp), loss of structural groups, decomposition or melting (indicated by a *black* circle)

(1) loss of water,
(2) pyrolysis of the organic matrix, and
(3) decarbonization and decomposition.

TG-MS and solid phase FTIR study of different bone samples dried in vacuum show removal of water from 50 to about 260 °C [105, 106]. This is in accordance with ^{1}H NMR results by Wilson who calcined bone to 225 °C and observed water in two crystal lattice environments [56].

The organic component of bone is pyrolyzed (combustion products are mainly water and CO_2 in air) up to 600 °C [105, 108, 111]. Newly formed phases appear beyond 400 °C, and include β-TCP, $NaCaPO_4$, NaCl and KCl.

The carbonate in bone is much more labile than in enamel and well-crystallized precipitated CO_3Ap [3]. Carbon dioxide already released at 150 °C continues up to 900–1000 °C with different intensities depending on the source of the sample. Carbonate is lost more quickly in forming and maturing enamel, compared to the mature enamel, giving a final weight loss at 800 °C.

A detailed study of calcined dental enamel samples using FTIR spectra revealed the replacement of carbonate ions in the apatite structure from B to A-type over molecular CO_2 and formation of β-TCP above 700 °C arising from the evolution of CO_2. The A-type carbonate shows a weak decrease below 300 °C. Further heating produces a systematic loss up to 700 °C. The B-type carbonate, however, shows a continuous weight loss. The loss of A-carbonate may commence at 100 °C, followed by a continuous weight loss [107].

The original placement of HAp within the collagen matrix is progressively lost, producing a porous HAp at 700 °C, and a very low porosity HAp product at 900 °C [108]. Carbonate evolution is similar with the synthetic CO_3Ap but depends on the type of sample, particularly on F content.

The complexity of changes upon heating biological apatites and the interest in producing a similar structure has placed focus on low temperature processing routes. Spark plasma sintering is a recently introduced technology, which uses sintering under pressure, and plasma sintering, that has successfully produced densified bodies at lower temperatures thereby avoiding the phase transformations that normally occur upon heating [112].

Concluding remarks and future potential

The chemical flexibility of the apatite structure allows many structural modifications to provide new properties. This has caused problems in the past where research articles do not provide the chemical purity of synthesized apatites, but show a variation in the properties compared to that reported by others. Both an improved knowledge of apatite characterization and new processing capabilities will play an important role in the development of apatites. Weight loss occurs from both the surface and the internal structure. Better understanding will be gained from a well-characterized surface and structure, whilst combining evolved gas analysis with thermal analysis techniques.

The thermal stability and the transitions involving loss of water, carbonate and decomposition are summarized in Fig. 4. This shows that substitution of carbonate leads to thermal instability, accentuating the need to minimize carbonate if thermal stability is required. From the different apatites, FAp is the most stable, followed by chlorapatite and then hydroxyapatite.

Synthetic apatites and bioapatites release water from their structure upon heating to 500–600 °C. This causes reorganization of the apatite structure, in the case of

carbonate substitution, with carbonate moving from the B-position to the hexagonal axis, and a release of some CO_2.

Heating to 600–1000 °C refines the lattice, removes most additives from synthesis, to create a more regular apatite. Carbonate and sulphate located in the phosphate position are evolved. The exact temperatures depend mainly on the F-OH ion proportion in apatite. A fluoride content favours a more regular apatite structure and accordingly dislodges substitutional groups. Therefore, the thermal stability of CO_3-Aps depends strongly on their exact chemical composition. Bioapatites are the most complex compositionally, and have a complex thermal behaviour. The thermal events are not completely understood, requiring further study.

Dehydroxylation and defluoridation starts at about 800–900 °C, Fig. 4. This is a continuous process that ends at about 1360 °C at atmospheric pressure with decomposition to calcium tetraphosphate and tri-calcium phosphate mixture. In the CaO-P_2O_5 system with a $Ca/P = 1.67$, an atmosphere containing the same halogen as in the structure (OH, F or CO_2) can stabilize the apatite until higher temperatures, Fig. 4. Thermal stability is lowered by inclusion of additives that form more stable phosphates or calcium compounds.

An analysis of the published results of apatite thermal stability shows that

- A substitution of phosphate decreases the decomposition temperature leading to a secondary phase and a more stoichiometric apatite.
- The thermal stability increases if the phosphate substitution is compensated with a substitution of calcium.
- Substitution of calcium with other metal ions decreases the thermal stability as the deformation in the structure increase; a greater difference in the cation size from calcium probably leads to a lower decomposition temperature.

Non-equilibrium heating and cooling can produce crystalline phases for which the thermal stability has not been determined. This includes the recrystallized fraction in plasma sprayed coatings. The lack of studies in this area is due to inability to locate and characterize the recrystallized phase. Most of the attention has been placed on crystallization of the amorphous phase, both in air and an atmosphere with steam.

Acknowledgements KT was supported by target financing by the MES of Estonia (Project No SF0140082s08) and the Estonian Science Foundation Grants No. 8207; KAG received support from the Marie Curie grant PIRG05-GA-2009-249306, and jointly with LP from an ESF grant # 2009/0199/1DP/1.1.1.2.0/09/APIA/VIAA/090.

References

1. Pan Y, Fleet ME. Compositions of the apatite group minerals: substitution mechanisms and controlling factors. In: Kohn MJ, Rakovan J, Hughes JM, editors. Phosphates: geochemical, geobiological and material importance. 2002. p. 13–50.
2. Pasero M, Kampf AR, Ferraris C, Pekov IV, Rakovan J, White TJ. Nomenclature of the apatite supergroup minerals. Eur J Mineral. 2010;22:163–79.
3. Elliott J. Structure and chemistry of the apatites and other calcium orthophosphates. Amsterdam: Elsevier; 1994.
4. Kanazawa T. Inorganic phosphates materialls. Tokyo: Kodansha Ltd. and Elsevier; 1989.
5. Gross KA, Berndt CC. Biomedical application of apatites. Phosphates: geochemical, geobiological and material importance. Rev Mineral Geochem. 2002;48:631–72.
6. Veiderma M. Studies on thermochemistry and thermal processing of apatite. Proc Estonian Acad Sci Chem. 2000;49:5–18.
7. Elliott JC. Calcium phosphate biominerals. Phosphates: geochemical, geobiological and material importance. Rev Mineral Geochem. 2002;48:427–54.
8. LeGeros R. Calcium phosphates in oral biology and medicine. New York: Karger Publishing; 1991.
9. Piccoli P, Candela P. Apatite in igneous systems. In: Kohn MJ, Rakovan J, Hughes JM, editors. Phosphates: geochemical, geobiological and material importance. Washington: Mineralogical Society of America; 2002. p. 255–92.
10. Cisse L, Mrabet T. World phosphate production: overview and prospects. Phosphorus Research Bulletin: Casablanca; 2004. p. 21–25.
11. Jasinski SM. Phosphate rock. In: Mineral Commodity Summaries. Washington, DC: U.S. Geological Survey; 2011. p. 118–9.
12. Marshall HL, Reynolds DS, Jacob KD, Tremearne TH. Phosphate fertilizers by calcination process. Ind Eng Chem. 1937; 29:1294–8.
13. Volfkovich SI, Veiderma M. The progress of hydrothermal processing of phosphate rock. In: Technical-economic conference. ISMA, Fertliser Techn Orlando: Orlando; 1978. p. 49–62.
14. Veiderma M, Knubovets R, Tõnsuaadu K. Fluorhydroxyapatites of Northern Europe and their thermal transformations. Phosphorus Sulfur Silicon Relat Elem. 1996;109:43–6.
15. Veiderma M, Pyldme M, Tynsuaadu K. Thermische entfluorierung of apatit. Chein Techn. 1988;40:169–72.
16. Sneddon IR, Orueetxebarria M, Hodson ME, Schofield PF, Valsami-Jones E. Use of bone meal amendments to immobilise Pb, Zn and Cd in soil: a leaching column study. Environ Pollut. 2006;144:816–25.
17. Lazic S, Zec S, Miljevic N, Milonjic S. The effect of temperature on the properties of hydroxyapatite precipitated from calcium hydroxide and phosphoric acid. Thermochim Acta. 2001; 374:13–22.
18. Dorozhkin SV. Calcium orthophosphate-based biocomposites and hybrid biomaterials. J Mater Sci. 2009;44:2343–87.
19. Gross KA, Berndt CC, Stephens P, Dinnebier R. Oxyapatite in hydroxyapatite coatings. J Mater Sci. 1998;33:3985–91.
20. Zyman Z, Ivanov I, Rochmistrov D, Glushko V, Tkachenko N, Kijko S. Sintering peculiarities for hydroxyapatite with different degrees of crystallinity. J Biomedical Mater Res. 2001;54: 256–63.
21. Ruys AJ, Wei M, Sorrell CC, Dickson MR, Brandwood A, Milthorpe BK. Sintering effects on the strength of hydroxyapatite. Biomater. 1995;16:409–15.
22. Haines P. Thermal methods of analysis. Principles, applications and problems. London: Blackie Academic & Professional; 1995.

23. Venkateswarlu K, Chandra Bose A, Rameshbabu N. X-ray peak broadening studies of nanocrystalline hydroxyapatite by Williamson-Hall analysis. Physica B. 2010;405:4256–61.
24. Wallaeys R. Contribution a l'etude des apatits phosphocalciques. Ann Chim. 1952;7:808–48.
25. Tanaka H, Chikazawa M, Kandori K, Ishikawa T. Influence of thermal treatment on the structure of calcium hydroxyapatite. Phys Chem Chem Phys. 2000;2:2647–50.
26. Dzyuba ED, Sokolov TM, Valyukevich PL. Thermal stability of calcium phosphates. Izvestiya Akad Nauk SSSR Neorg Mater. 1982;18:107–10 (In russian).
27. Prener JS. The growth and crystallographic properties of calcium fluor- and chlorapatite crystals. J Electrochem Soc. 1967;114:77–83.
28. Surendran R, Chinnakali K. Preparation and characterisation of fluorapatite whiskers. Cryst Res Technol. 2008;43:490–5.
29. Demnanti I, Grossin D, Combes C, Rey C, Parco M, Fagoaga I, Barykin G, Braceras I. Hydroxyapatite and chlorapatite. Thin coatings obtained by a novel plasma mini-torch process. In: 5th forum on new materials. Nantes; 2010, p. FL-1–L-14.
30. Kannan S, Rebelo A, Lemos AF, Barba A, Ferreira JMF. Synthesis and mechanical behaviour of chlorapatite and chlorapatite/β-TCP composites. J Eur Ceram Soc. 2007;27:2287–94.
31. García-Tuñón E, Franco J, Dacuña B, Zaragoza G, Guitián F. Chlorapatite conversion to hydroxyapatite under high temperature hydrothermal conditions. Mater Sci Forum. 2010;636–637:9–14.
32. Liao C-J, Lin F-H, Chen K-S, Sun J-S. Thermal decomposition and reconstitution of hydroxyapatite in air atmosphere. Biomater. 1999;20:1807–13.
33. Park HC, Baek DJ, Park YM, Yoon SY, Stevens R. Thermal stability of hydroxyapatite whiskers derived from the hydrolysis of α-TCP. J Mater Sci. 2004;39:2531–4.
34. Wang T, Dorner-Reisel A, Müller E. Thermogravimetric and thermokinetic investigation of the dehydroxylation of a hydroxyapatite powder. J Eur Ceram Soc. 2004;24:693–8.
35. Ivanova TI, Frank-Kamenetskaya OV, Kol'tsov AB, Ugolkov VL. Crystal structure of calcium-deficient carbonated hydroxyapatite. Thermal decomposition. J Solid State Chem. 2001;160:340–9.
36. Corno M, Busco C, Bolis V, Tosoni S, Ugliengo P. Water adsorption on the stoichiometric (001) and (010) surfaces of hydroxyapatite: a periodic B3LYP study. Langmuir. 2009;25:2188–98.
37. Sakhno Y, Bertinetti L, Iafisco M, Tampieri A, Roveri N, Martra G. Surface hydration and cationic sites of nanohydroxyapatites with amorphous or crystalline surfaces: a comparative study. J Phys Chem C. 2010;114:16640–8.
38. Wang PE, Chaki TK. Sintering behaviour and mechanical properties of hydroxyapatite and dicalcium phosphate. J Mater Sci. 1993;4:150–8.
39. Chen Y, Miao X. Thermal and chemical stability of fluorohydroxyapatite ceramics with different fluorine contents. Biomater. 2005;26:1205–10.
40. White AA, Kinloch IA, Windle AH, Best SM. Optimization of the sintering atmosphere for high-density hydroxyapatite -carbon nanotube composites. J R Soc Interface. 2010;7:S529–39.
41. Bredig MA, Frank HH, Füldner H. Beiträge zur kenntnis der kalk-phosphorsäure-verbindungen II. Z Elektrochem. 1933;39:959–69.
42. Trombe JC, Montel G. Some features of the incorporation of oxygen in different oxidation states in the apatitic lattice–I on the existence of calcium and strontium oxyapatites. J Inorg Nucl Chem. 1978;40:15–21.
43. Cihlář J, Buchal A, Trunec M. Kinetics of thermal decomposition of hydroxyapatite bioceramics. J Mater Sci. 1999;34:6121–31.
44. Fowler BO. Infrared studies of apatites. I. Vibrational assignments for calcium, strontium, and barium hydroxyapatites utilizing isotopic substitution. Inorg Chem. 1974;13:194–207.
45. Monma H, Kanazawa T. Effect of hydroxylation on the thermal reactivities of fluorapatite and chlorapatite. Bull Chem Soc Jpn. 1976;49:1421–2.
46. Locardi B, Pazzaglia UE, Gabbi C, Profilo B. Thermal behaviour of hydroxyapatite intended for medical applications. Biomater. 1993;14:437–41.
47. Gross KA, Gross V, Berndt CC. Thermal analysis of amorphous phases in hydroxyapatite coatings. J Am Ceram Soc. 1998;81:106–12.
48. Chen J, Tong W, Yang C, Feng J, Zhang X. Efect of atmosphere on phase transformation in plasma-sprayed hydroxyapatite coatings during heat treatment. J Biomedical Mater Res. 1997;34:15–20.
49. Combes C, Rey C. Amorphous calcium phosphates: synthesis, properties and uses in biomaterials. Acta Biomater. 2010;6:3362–78.
50. McPherson R, Gane N, Bastow TJ. Structural characterization of plasma-sprayed hydroxylapatite coatings. J Mater Sci. 1995;6:327–34.
51. Yang C-W, Lui T-S. Kinetics of hydrothermal crystallization under saturated steam pressure and the self-healing effect by nanocrystallite for hydroxyapatite coatings. Acta Biomater. 2009;5:2728–37.
52. Lin F-H, Chun-Jen L, Ko-Shao C, Jui-Sheng S. Thermal reconstruction behavior of the quenched hydroxyapatite powder during reheating in air. Mater Sci Eng. 2000;13:97–104.
53. Shpak AP, Karbovskii VL, Trachevskii VV. Apatites, Kiev: Akademperiodika; 2002. (In Russian).
54. Park E, Condrate RA, Lee D, Kociba K, Gallagher PK. Characterization of hydroxyapatite: before and after plasma spraying. J Mater Sci. 2002;13:211–8.
55. DeGroot K, Klein C, Wolke J, De Blieck-Hogervorst J. Calcium phosphate and hydroxylapatite ceramics. Plasma-sprayed coatings of calcium phosphate. In: Yamamuro T, Hench LL, Wilson J, editors. CRC handbook of bioactive ceramics. Boca Raton: CRC Press; 1990. p. 133–42.
56. Wilson R, Elliott J, Dowker S, Rodriguez-Lorenzo L. Rietveld refinements and spectroscopic studies of the structure of Ca-deficient apatite. Biomaterials. 2005;26:1317–27.
57. Raynaud S, Champion E, Bernache-Assollant D, Thomas P. Calcium phosphate apatites with variable Ca/P atomic ratio I. Synthesis, characterisation and thermal stability of powders. Biomaterials. 2002;23:1065–72.
58. Gibson IR, Bonfield W. Novel synthesis and characterization of an AB-type carbonate-substituted hydroxyapatite. J Biomed Mater Res. 2002;59:697–708.
59. Astala R, Stott MJ. First principles investigation of mineral component of bone: CO_3 substitutions in hydroxyapatite. Chem Mater. 2005;17:4125–33.
60. Li Y, Kong F, Weng W. Preparation and characterization of novel biphasic calcium phosphate powders (α-TCP/HA) derived from carbonated amorphous calcium phosphates. J Biomedical Mater Res Part B. 2009;89B:508–17.
61. Kim KY, Shaver KJ. Calcination properties of precipitated basic calcium phosphates. J KIChE. 1973;11:336–48.
62. Pyldme M, Buzágh-Gere É, Pyldme J, Veiderma M. Thermal analysis of the interaction of phosphorite with condensed phosphates of calcium. J Therm Anal Calorim. 1976;10:195–204.
63. Nilen R, Richter P. The thermal stability of hydroxyapatite in biphasic calcium phosphate ceramics. J Mater Sci. 2008;19:1693–702.

64. DeLeeuw NH. Computer simulations of structures and properties of the biomaterial hydroxyapatite. J Mater Chem. 2010;20: 5376–89.
65. Zyman Z, Rokhmistrov D, Glushko V, Ivanov I. Thermal impurity reactions and structural changes in slightly carbonated hydroxyapatite. J Mater Sci. 2009;20:1389–99.
66. Bonel G. Contribution à l'étude de la carbonation des apatites - 1- Synthèse et étude des propriétés physico-chimiques des apatites carbonatées du type A. Ann Chim Fr. 1972;7:65–88.
67. Lafon JP, Champion E, Bernache-Assollant D. Processing of AB-type carbonated hydroxyapatite $Ca_{10-x}(PO_4)_{6-x}(CO_3)_x(OH)_{2-x-2y}(CO_3)_y$ ceramics with controlled composition. J Eur Ceram Soc. 2008;28:139–47.
68. Tõnsuaadu K, Peld M, Leskelä T, Mannonen R, Niinistö L, Veiderma M. A thermoanalytical study of synthetic carbonate-containing apatites. Thermochim Acta. 1995;256:55–65.
69. Krajewski A, Mazzocchi M, Buldini PL, Ravaglioli A, Tinti A, Taddei P, Fagnano C. Synthesis of carbonated hydroxyapatites: efficiency of the substitution and critical evaluation of analytical methods. J Mol Struct. 2005;744–747:221–8.
70. Tadic D, Epple M. A thorough physicochemical characterisation of 14 calcium phosphate-based bone substitution materials in comparison to natural bone. Biomater. 2004;25:987–94.
71. Lafon J, Champion E, Bernache-Assollant D, Gibert R, Danna A. Termal decomposition of carbonated calcium phosphate apatites. J Therm Anal Calorim. 2003;72:1127–34.
72. Tõnsuaadu K, Peld M, Bender V. Thermal analysis of apatite structure. J Therm Anal Calorim. 2003;72:363–71.
73. Zhu Q, Wu J. Effect of initial carbonate content and heat treatments on preparation and properties of carbonated hydroxyapatite. J Chinese Ceramic Soc. 2007;35:866–70.
74. Zhu QX, Wu JQ. Investigation on heat treatment of carbonated hydroxyapatite. J Funct Mater. 2007;38:2055–8.
75. Barralet J, Knowles JC, Best S, Bonfield W. Thermal decomposition of synthesised carbonate hydroxyapatite. J Mater Sci. 2002;13:529–33.
76. Rau J, Cesaro SN, Ferro D, Barinov S, Fadeeva I. FTIR study of carbonate loss from carbonated apatites in the wide temperature range. J Biomed Mater Res Part B. 2004;71B:441–7.
77. Vignoles M, Bonel G, Bacquet G. Physicochemical study on phosphocalcium carbonated apatites similar to francolite. Bull Mineral. 1982;105:307–11.
78. Perdikatsis B. X-ray powder diffraction study of francolite by the Rietveld method. Mater Sci Forum. 1991;79–82:809–14.
79. McClellan G, Van Kauwenbergh S. Mineralogy of sedimentary apatites. In: Phosphorite research and development. London: Geological Society; 1990. p. 23–31.
80. Jemal M, Khattech I. Simultaneous thermogravimetry and gas chromatography during decomposition of carbonate apatites. Thermochim Acta. 1989;152:65–76.
81. Callens FJ, Verbeeck RMH, Naessens DE, Matthys PFA, Boesman ER. The effect of carbonate content and drying temperature on the ESR-spectrum near $g = 2$ of carbonated calciumapatites synthesized from aqueous media. Calcif Tissue Int. 1991;48:249–59.
82. Bianco A, Cacciotti I, Lombardi M, Montanaro L, Bemporad E, Sebastiani M. F-substituted hydroxyapatite nanopowders: thermal stability, sintering behaviour and mechanical properties. Ceram Int. 2010;36:313–22.
83. Tõnsuaadu K, Peld M, Quarton M, Bender V, Veiderma M. Studies on SO_4^{2-} ion incorporation into apatite structure. Phosphorus, Sulfur, Silicon Relat Elem. 2002;177:1873–6.
84. Khattech I, Jemal M. Décomposition thermique de fluorapatites carbonatées de type b "inverses". Thermochim Acta. 1987;118: 267–75.
85. Slósarczyk A, Paszkiewicz Z, Paluszkiewicz C. FTIR and XRD evaluation of carbonated hydroxyapatite powders synthesized by wet methods. J Mol Struct. 2005;744–747:657–61.
86. Kannan S, Ventura JMG, Lemos AF, Barba A, Ferreira JMF. Effect of sodium addition on the preparation of hydroxyapatites and biphasic ceramics. Ceram Int. 2008;34:7–13.
87. Leskiv M, Lagoa ALC, Urch H, Schwiertz J, Da Piedade Minas ME, Epple M. Energetics of calcium phosphate nanoparticle formation by the reaction of $Ca(NO_3)_2$ with $(NH_4)_2HPO_4$. J Phys Chem C. 2009;113:5478–84.
88. Yasukawa A, Kandori K, Ishikawa T. TPD-TG-MS study of carbonate calcium hydroxyapatite particles. Calcif Tissue Int. 2003;72:243–50.
89. Hidouri M, Bouzouita K, Kooli F, Khattech I. Thermal behaviour of magnesium-containing fluorapatite. Mater Chem Phys. 2003;80:496–505.
90. Ren F, Leng Y, Xin R, Ge X. Synthesis, characterization and ab initio simulation of magnesium-substituted hydroxyapatite. Acta Biomater. 2010;6:2787–96.
91. Marchi J, Dantas ACS, Greil P, Bressiani JC, Bressiani AHA, Müller FA. Influence of Mg-substitution on the physicochemical properties of calcium phosphate powders. Mater Res Bull. 2007;42:1040–50.
92. Cacciotti I, Bianco A, Lombardi M, Montanaro L. Mg-substituted hydroxyapatite nanopowders: synthesis, thermal stability and sintering behaviour. J Eur Ceram Soc. 2009;29:2969–78.
93. Medveckż L, Stulajterovį R, Parilįk L, Trpcevskį J, Durisin J, Barinov SM. Influence of manganese on stability and particle growth of hydroxyapatite in simulated body fluid. Coll Surfaces A. 2006;281:221–9.
94. Paluszkiewicz C, Slósarczyk A, Pijocha D, Sitarz M, Bucko M, Zima A, Chróscicka A, Lewandowska-Szumiel M. Synthesis, structural properties and thermal stability of Mn-doped hydroxyapatite. J Mol Struct. 2010;976:301–9.
95. Li MO, Xiao X, Liu R, Chen C, Huang L. Structural characterization of zinc-substituted hydroxyapatite prepared by hydrothermal method. J Mater Sci. 2008;19:797–803.
96. Costa AM, Soares GA, Calixto R, Rossi AM. Preparation and properties of zinc containing biphasic calcium phosphate bioceramics. Key Eng Mater. 2004;254–256:119–22.
97. Loher S, Stark WJ, Maciejewski M, Baiker A, Pratsinis SE, Reichardt D, Maspero F, Krumeich F, Günther D. Fluoro-apatite and calcium phosphate nanoparticles by flame synthesis. Chem Mater. 2004;17:36–42.
98. Riad M, Mikhail S. Zinc incorporated hydroxyapatite as catalysts for oxidative desulphurization process. Glob J Res in Eng. 2010;10:85–91.
99. Guerra-López J, Pomés R, Védova COD, Viña R, Punte G. Influence of nickel on hydroxyapatite crystallization. J Raman Spectrosc. 2001;32:255–61.
100. Bigi A, Gazzano M, Ripamonti A, Foresti E, Roveri N. Thermal stability of cadmium-calcium hydroxyapatite solid solutions. J Chem Soc Dalton Trans. 1986; 241–4.
101. Nounah A, Lacout JL. Thermal behavior of cadmium-containing apatites. J Solid State Chem. 1993;107:444–51.
102. Silva GWC, Hemmers O, Czerwinski KR, Lindle DW. Investigation of nanostructure and thermal behavior of zinc-substituted fluorapatite. Inorg Chem. 2008;47:7757–67.
103. Pasteris JD, Wopenkaa B, Freemana J, Rogersb K, Valsami-Jonesc E, van der Houwenc J, Silvad M. Lack of OH in nanocrystalline apatite as a function of degree of atomic order: implications for bone and biomaterials. Biomaterials. 2004;25:229–38.
104. Loong CK, Rey C, Kuhn LT, Combes C, Wu Y, Chen SH, Glimcher MJ. Evidence of hydroxyl-ion deficiency in bone apatites: an inelastic neutron-scattering study. Bone. 2000;26: 599–602.

105. Peters F, Schwarz K, Epple M. The structure of bone studied with synchrotron X-ray diffraction, X-ray absorption spectroscopy and thermal analysis. Thermochim Acta. 2000;361:131–8.
106. Shi J, Klocke A, Zhang M, Bismayer U. Thermal behavior of dental enamel and geologic apatite: An infrared spectroscopic study. Am Mineral. 2003;88:1866–71.
107. Shi J, Klocke A, Zhang M, Bismayer U. Thermally-induced structural modification of dental enamel apatite: decomposition and transformation of carbonate groups. Eur J Mineral. 2005; 17:769–75.
108. Etok S, Valsami-Jones E, Wess T, Hiller J, Maxwell C, Rogers K, Manning D, White M, Lopez-Capel E, Collins M, Buckley M, Penkman K, Woodgate S. Structural and chemical changes of thermally treated bone apatite. J Mater Sci. 2007;42:9807–16.
109. Rabelo JS, Ana PA, Benetti C, Valerio MEG, Zezell DM. Changes in dental enamel oven heated or irradiated with Er, Cr:YSGG laser. Analysis by FTIR. Laser Phys. 2010;20:871–5.
110. Barralet J, Best SM, Bonfield W. Effect of sintering parameters on the density and microstructure of carbonate hydroxyapatite. J Mater Sci. 2000; 19–24.
111. Onishi A, Thomas P, Stuart B, Guerbois J, Forbes S. TG-MS analysis of the thermal decomposition of pig bone for forensic applications. J Therm Anal Calorim. 2008;92:87–90.
112. Grossin D, Rollin-Martinet S, Estournčs C, Rossignol F, Champion E, Combes C, Rey C, Geoffroy C, Drouet C. Biomimetic apatite sintered at very low temperature by spark plasma sintering: Physico-chemistry and microstructure aspects. Acta Biomater. 2010;6:577–85.